

# Distinct Subcellular Trafficking Resulting from Monomeric vs Multimeric Targeting to Endothelial ICAM-1: Implications for Drug Delivery

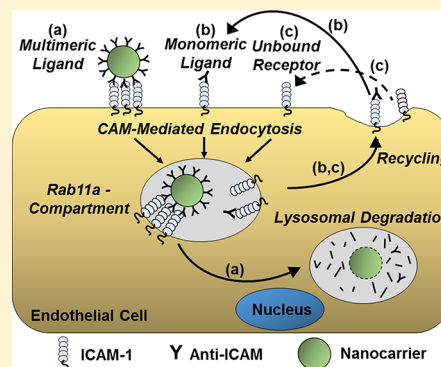
Rasa Ghaffarian<sup>†</sup> and Silvia Muro<sup>\*,†,‡</sup>

<sup>†</sup>Fischell Department of Bioengineering, University of Maryland, 2330 Jeong H. Kim Engineering Building, College Park, Maryland 20742, United States

<sup>‡</sup>Institute for Bioscience and Biotechnology Research, University of Maryland, 5115 Plant Sciences Building, College Park, Maryland 20742, United States

**ABSTRACT:** Ligand-targeted, receptor-mediated endocytosis is commonly exploited for intracellular drug delivery. However, cell-surface receptors may follow distinct endocytic fates when bound by monomeric vs multimeric ligands. Our purpose was to study this paradigm using ICAM-1, an endothelial receptor involved in inflammation, to better understand its regulation and potential for drug delivery. Our procedure involved fluorescence microscopy of human endothelial cells to determine the endocytic behavior of unbound ICAM-1 vs ICAM-1 bound by model ligands: monomeric (anti-ICAM) vs multimeric (anti-ICAM biotin-streptavidin conjugates or anti-ICAM coated onto 100 nm nanocarriers). Our findings suggest that both monomeric and multimeric ligands undergo a similar endocytic pathway sensitive to amiloride (~50% inhibition), but not inhibitors of clathrin-pits or caveoli. After 30 min, ~60–70% of both ligands colocalized with Rab11a-compartments. By 3–5 h, ~65–80% of multimeric anti-ICAM colocalized with perinuclear lysosomes with ~60–80% degradation, while 70% of monomeric anti-ICAM remained associated with Rab11a at the cell periphery and recycled to and from the cell-surface with minimal (<10%) lysosomal colocalization and minimal ( $\leq 15\%$ ) degradation. In the absence of ligands, ICAM-1 also underwent amiloride-sensitive endocytosis with peripheral distribution, suggesting that monomeric (not multimeric) anti-ICAM follows the route of this receptor. In conclusion, ICAM-1 can mediate different intracellular itineraries, revealing new insight into this biological pathway and alternative avenues for drug delivery.

**KEYWORDS:** CAM-mediated endocytosis, intracellular trafficking, receptor-mediated endocytosis, targeted drug carriers, vascular endothelium



## INTRODUCTION

Endocytosis of cell surface receptors mediates a wide range of physiological functions, including cellular uptake of nutrients, signal transduction, recycling of membrane components, and clearance of foreign or pathogenic elements.<sup>1,2</sup> Also, from a translational perspective, receptor-mediated endocytosis is commonly exploited in order to achieve delivery of diagnostic or therapeutic agents within cells.<sup>3</sup> Under both scenarios, specific endocytic processes are initiated upon binding of an extracellular affinity molecule (the ligand) to its respective cell surface receptor.<sup>2,3</sup> The binding event induces signaling cascades conducive to recruitment of partner proteins and/or coats, which, along with other changes, result in the engulfment of the ligand–receptor complex into vesicles that bud off into the cell.<sup>2,4</sup> When exploited for intracellular drug delivery, receptor-mediated endocytosis is achieved using natural ligands of a designated receptor (hormones, vitamins, lectins, etc.), ligands derived from pathogens (viral binding sites, bacterial toxins, etc.), or “artificial” ligands generated for this purpose (antibodies and their fragments, synthetic peptides, aptamers, etc.).<sup>3,5</sup> In all cases,

the selected ligand is either coupled to a pharmaceutical agent of interest (drug conjugates) or coated on the surface of submicrometer drug delivery systems (nanocarriers; NCs), which contain said agent, such as the case of liposomes, micelles, dendrimers, polymer particles, etc.<sup>6</sup>

Both receptor-targeting conjugates and carriers are valuable, yet it is expected that they would significantly differ in their ligand–receptor interactions and, therefore, subsequent endocytic events.<sup>5</sup> An important example pertains to the valency of such ligand–receptor engagement: a small drug conjugate typically involves interaction of one ligand with one receptor (or two if a divalent antibody is used), while larger drug conjugates and NCs employ multiple copies of a ligand to engage multiple copies of a cell surface receptor.<sup>5</sup> In nature, receptors typically bind to either monomeric or multimeric ligands, but rarely both.<sup>2</sup>

Received: June 9, 2014

Revised: September 16, 2014

Accepted: October 9, 2014

Published: October 9, 2014

As a consequence, drug targeting to endocytic receptors does not guarantee a similar uptake efficacy or mechanism to that of natural, unmodified ligands of said receptors, as observed in several studies.<sup>7–10</sup> This is also the case with regard to intracellular routing after endocytosis: some receptors may follow more than one itinerary (e.g., to lysosomes, recycling compartments, transcytosis, etc.), which further depends on whether they are bound by natural or artificial ligands, or by monomeric vs multimeric counterparts, as observed for receptors of immunoglobulins, transferrin, and folate, for instance.<sup>7,8,11–13</sup> Therefore, understanding the endocytic fate of ligands employed for drug delivery is important in order to determine the efficacy of these strategies and the selection of suitable therapeutic applications, while also providing insight on the biological regulation of their cell surface receptors.

Most previous studies comparing the endocytic fates of drug targeting platforms using natural ligands have examined receptors whose said natural ligands are monomeric (transferrin, folate, aminopeptidase A, etc.).<sup>7,8,10</sup> There are fewer studies available regarding receptors whose natural ligands are multimeric. Perhaps one of the examples where more mechanistic information is available is that of drug targeting to intercellular adhesion molecule-1 (ICAM-1).<sup>14–18</sup> ICAM-1 is a cell surface molecule involved in inflammation and preferentially expressed on vascular endothelial cells subjected to pathological factors.<sup>19</sup> As such, ICAM-1 is being explored as a target for intervention against inflammation, immune disorders, cardiovascular disease, genetic and metabolic syndromes, and cancers, among other conditions.<sup>20–29</sup> Previous studies on ICAM-1 targeting using antibodies or peptides revealed that this molecule undergoes more efficient endocytosis when bound in a multimeric manner, as opposed to a monomeric manner.<sup>9,14,20</sup> This pairs well with the fact that natural ligands of ICAM-1 bind this molecule in a multimeric fashion, including leukocytes, apoptotic bodies, plasmodium-infected erythrocytes, pathogens such as major class rhinoviruses, etc.<sup>30–34</sup>

While endocytosis of monomeric ligands targeting ICAM-1 did not seem prominent a priori,<sup>20</sup> their pathway of uptake has not been examined. In addition, certain plasmalemma receptors can be internalized in the absence of ligand binding, and their intracellular itinerary can differ from that of the ligand–receptor complex,<sup>13,35,36</sup> yet potential endocytosis of unbound ICAM-1 also remains largely unexplored. Indeed, ICAM-1 has been observed to recycle back to the cell surface after separating from ligands in endocytic compartments,<sup>15</sup> a phenomenon that seems reminiscent of the continuous redistribution of ICAM-1 between the cell surface and an intracellular pool in certain immune cells.<sup>37</sup>

In this report, we have studied endocytosis and subsequent routing of the unbound vs ligand-bound receptor (using monomeric vs multimeric ligands) to shed light on the biological regulation of ICAM-1 and its utility for diverse therapeutic applications.

## ■ EXPERIMENTAL SECTION

**Antibodies and Reagents.** Mouse monoclonal antibody to human ICAM-1 (anti-ICAM) was clone R6.5 (American Type Culture Collection; Manassas, VA, USA). Fluoresbrite 100 nm diameter polystyrene particles were from Polysciences (Warrington, PA, USA). Rabbit polyclonal antibody against human lysosomal-associated membrane protein 1 (LAMP-1), as well as FITC- and Texas Red (TxR)-labeled secondary antibodies were from Jackson ImmunoResearch (West Grove, PA, USA). Goat polyclonal antibody against human Rab11a was

from Abcam (Cambridge, MA, USA). Green Alexa Fluor 488-labeled streptavidin, TxR dextran, blue Alexa Fluor 350-labeled secondary antibodies, and FluoReporter FITC Protein Labeling Kit were from Invitrogen (Grand Island, NY, USA). Unless otherwise stated, all other reagents were from Sigma-Aldrich (St. Louis, MO, USA).

**Cell Culture.** Human umbilical vein endothelial cells (HUVECs) from Clonetics (San Diego, CA, USA) were grown in M199 medium (GibcoBRL, Grand Island, NY, USA) supplemented with 15% fetal bovine serum, 2 mM glutamine, 15 mg/mL endothelial cell growth supplement, 100 mg/mL heparin, 100 U/mL penicillin, and 100 mg/mL streptomycin. Cell cultures were maintained at 37 °C, 5% CO<sub>2</sub>, and 95% relative humidity. Cells between passages 4 and 5 were seeded onto 12 mm diameter gelatin-coated coverslips in 24-well plates and treated with 10 ng/mL tumor necrosis factor-alpha (TNF-α; BD Biosciences, Franklin Lakes, NJ, USA) for 16 h to mimic a pathological-like status. Overexpression of ICAM-1 and, hence, increased binding of ICAM-1-ligands upon TNF-α-activation, in accord with a pathological state, have been previously confirmed.<sup>9,14,20,38</sup>

**Preparation of Multimeric Anti-ICAM NCs.** Anti-ICAM or nonspecific IgG were coated onto 100 nm diameter green Fluoresbrite polystyrene particles to render anti-ICAM nanocarriers (anti-ICAM NCs) or IgG NCs, as previously described.<sup>9</sup> Briefly, 5 μM antibody was incubated with ~10<sup>13</sup> particles/mL for 1 h at room temperature to allow adsorption of the antibody on the particle surface. Noncoated antibody was removed by centrifugation at 13.8g for 3 min and coated carriers were resuspended at ~7 × 10<sup>11</sup> NCs/mL in 1% bovine serum albumin (BSA)-supplemented phosphate buffered saline and sonicated to remove aggregates. Characterization of anti-ICAM NCs revealed a hydrodynamic diameter of 152 ± 58 nm, as determined by nanoparticle tracking analysis (NanoSight LM10, Malvern Instruments, Westborough, MA). The polydispersity index was 0.220 ± 0.048 and the ζ-potential was -27 ± 5 mV, as determined by dynamic light scattering (Zetasizer NanoZS90, Malvern Instruments, Westborough, MA). Antibody surface-coating was 208.3 ± 42.7 antibodies per carrier, as determined by radioisotope quantification using <sup>125</sup>I-labeled anti-ICAM, as described.<sup>9</sup> Control IgG NCs had a diameter of 158 ± 5 nm, polydispersity index of 0.19 ± 0.03, ζ-potential of -31 ± 2 mV, and 176 ± 8 antibodies per carrier.

Validating this model, previous studies have demonstrated that these anti-ICAM NCs do not suffer changes in fluorescence intensity under conditions reflective of intracellular compartments and do not undergo apparent aggregation, antibody detachment (in storage or physiological media), or coating with serum proteins (albumin).<sup>21,39</sup> This formulation, although not suitable for clinical studies, is an adequate model for this work because of high reproducibility of the coating density and other parameters described above.<sup>9,17,21,38–40</sup> Each independent batch of carriers displays a similarly random orientation of the adsorbed antibodies which leads to this reproducibility. This is similar to the variability of chemical conjugation techniques, where the precise amino acid residue being modified and, hence, the final orientation varies for each antibody in the population. The fact that similar binding, uptake, intracellular trafficking, and *in vivo* biodistribution of anti-ICAM NCs have been reported from many different studies validates the batch-to-batch reproducibility of this model formulation.<sup>9,17,21,38–40</sup> Moreover, this model has also shown similar binding, endocytosis, intracellular trafficking, and *in vivo* circulation and

biodistribution as biocompatible poly(lactic-*co*-glycolic acid) (PLGA) NCs.<sup>22,38</sup>

**Preparation of Multimeric Anti-ICAM Conjugates.** An alternative multimeric model lacking a polymer particle consisted of anti-ICAM protein conjugates. For this purpose, anti-ICAM was biotinylated at a 1:5 antibody-to-biotin molar ratio using 6-biotinylaminocaproic acid *N*-hydroxysuccinimide ester, as previously described.<sup>41</sup> Conjugation was performed by incubating biotinylated anti-ICAM with (green) Alexa Fluor 488-labeled streptavidin at 1:1 molar ratio for 1 h at 4 °C. This protocol rendered conjugates with hydrodynamic diameter of 323 ± 43 nm, polydispersity index of 0.429 ± 0.053, and a  $\zeta$ -potential of -4.0 ± 0.5 mV as determined by dynamic light scattering.

**Degree and Mechanism of Uptake of Monomeric vs Multimeric Anti-ICAM.** TNF- $\alpha$ -activated HUVECs were incubated with monomeric anti-ICAM (140 pM) or multimeric anti-ICAM NCs (36 pM antibody since this formulation has greater avidity vs anti-ICAM<sup>38</sup>) or conjugates (214 pM antibody) for 30 min in 1% BSA-supplemented cell medium to allow their binding to the cell surface (pulse period). Control experiments were performed using either nonspecific IgG or IgG NCs, or by incubating anti-ICAM conjugates in the presence of competing anti-ICAM. After this time, cell medium containing nonbound counterparts was removed, and cells were washed and incubated at 37 °C with fresh medium for the indicated time intervals, to allow internalization of surface-bound materials (chase period). In parallel, incubation at 4 °C served as a negative control for energy-dependent uptake. Alternatively, to evaluate the mechanism of uptake, incubations were performed in the presence of either 3 mM amiloride (an inhibitor of macropinocytosis and CAM-mediated endocytosis), 50  $\mu$ M monodansylcadaverine (MDC; inhibitor of clathrin-mediated endocytosis), 1  $\mu$ g/mL filipin (inhibitor of caveolar endocytosis), or 0.5  $\mu$ M wortmannin (inhibitor of phosphatidylinositol 3 kinase (PI3K), involved in macropinocytosis).<sup>14</sup>

All cell samples were then fixed with 2% paraformaldehyde for 15 min at room temperature. Surface-bound anti-ICAM, anti-ICAM NCs, or anti-ICAM conjugates were immunostained with TxR-labeled goat antimouse IgG for 1 h. Since polymer particles and streptavidin contain a green fluorescent label, all cell-associated anti-ICAM NCs and anti-ICAM conjugates are visible in the green channel while only surface-located counterparts fluoresce in the red channel, thus enabling differential visualization and quantification, as described.<sup>14,41</sup> In the case of monomeric anti-ICAM, after similarly immunostaining cell-surface counterparts in red, cells were permeabilized with 0.2% Triton X-100, followed by incubation with green FITC-labeled goat antimouse IgG, which would label all cell-associated anti-ICAM in green, thereby enabling similar distinction and quantification of cell-surface bound vs internalized counterparts by fluorescence microscopy. In both cases, in addition to endocytosis, the localization of anti-ICAM, anti-ICAM NCs, and anti-ICAM conjugates within 5  $\mu$ m of the cell nucleus (perinuclear) or within 5  $\mu$ m from the cell border (herein called periphery) was also quantified.

**Intracellular Trafficking of Monomeric vs Multimeric Anti-ICAM.** TNF- $\alpha$ -activated HUVECs were incubated with green FITC-labeled anti-ICAM, anti-ICAM on the surface of green Fluoresbrite carriers, or green Alexa Fluor 488-labeled anti-ICAM conjugates for a pulse of 30 min. Cells were then washed and incubated for up to 1, 3, or 5 h (37 °C) in the absence of a ligand, as described above. Cells were subsequently fixed and permeabilized, and lysosomes or recycling compartments were

immunostained with anti-LAMP-1 or anti-Rab11a, respectively, followed by TxR-labeled secondary antibodies. In the case of anti-ICAM conjugates, an additional lysosomal labeling method was used to avoid cell permeabilization and subsequent leakage of the fluorescent dye from degraded conjugates. Here, cells were pretreated with 10 kDa TxR dextran for 45 min at 37 °C, washed, and incubated with fresh medium for another 45 min at 37 °C prior to addition of anti-ICAM conjugates.<sup>42</sup> This protocol enables lysosomal trafficking of dextran, which allows visualization of this compartment due to the lack of dextran degradation by mammalian cells, as previously verified.<sup>42</sup> Colocalization of green-labeled anti-ICAM, anti-ICAM NCs, or anti-ICAM conjugates with each one of these red-labeled compartments (lysosomes or recycling endosomes) was calculated from fluorescence micrographs.<sup>42</sup> The number of endocytic vesicles containing monomeric or multimeric anti-ICAM and the number of LAMP-1 and dextran-labeled compartments were additionally quantified.

**Intracellular Degradation of Monomeric vs Multimeric Anti-ICAM.** Using the protocol described above, degradation of naked green FITC-labeled anti-ICAM or green Alexa Fluor 488-labeled anti-ICAM conjugates was estimated by comparing the total fluorescence remaining over time (chase incubation) to the cell-associated fluorescence achieved after the first 30 min incubation. Agents that have been previously shown to inhibit lysosomal trafficking via the CAM pathway, nocodazole (20  $\mu$ M),<sup>42</sup> or to inhibit activation of lysosomal hydrolases, chloroquine (300  $\mu$ M),<sup>42</sup> were used as controls for degradation. These agents were incubated with cells during the chase period only to preclude potential effects on uptake. In the case of green anti-ICAM NCs, cells were incubated with TxR goat antimouse IgG after permeabilization, to immunodetect anti-ICAM on the surface of internalized particles. Hence, lack of antibody degradation was visualized as colocalization of TxR-labeled anti-ICAM with green fluorescent particles, while degradation was observed as single-labeled green-particles. Time-dependent degradation of anti-ICAM on NCs was calculated by comparing the number of antibody-free particles to the total number of cell-associated particles, as described.<sup>42</sup>

**ICAM-1 Distribution and Recycling in the Absence of Ligands.** To examine potential transit of ICAM-1 between the cell-surface and intracellular vesicles, TNF- $\alpha$ -activated HUVECs were incubated with 10  $\mu$ g/mL cyclohexamide to inhibit *de novo* protein synthesis, which may confound results. After 1 h, cells were fixed and ICAM-1 expressed on the cell-surface was immunostained in red using anti-ICAM followed by TxR-labeled goat antimouse IgG. Cells were then permeabilized, and total cell-associated ICAM-1 (surface + intracellular) was labeled using anti-ICAM followed by green FITC goat antimouse IgG. Using this method, the percentage of green, single-labeled ICAM-1 that does not colocalize with double-labeled (FITC + TxR) ICAM-1 represents the intracellular fraction, which was quantified by fluorescence microscopy.

**Intracellular Trafficking of Unbound ICAM-1.** To assess endocytosis of ICAM-1 in the absence of ligands, TNF- $\alpha$ -activated HUVECs were incubated continuously for 30 min, 1, 3, or 5 h at 37 °C with 20  $\mu$ g/mL TxR-labeled tomato lectin to stain the cell surface. After different periods of time, cells were washed and fixed, and ICAM-1 located on the cell surface was stained in blue using anti-ICAM followed by blue Alexa Flour 350-goat antimouse IgG. Cells were then permeabilized, and total cell-associated anti-ICAM was labeled in green with anti-ICAM and FITC goat antimouse IgG. Using this method,

surface-located ICAM-1 should colocalize with lectin and appear white (green FITC + red TxR + blue Alexa Fluor 350), while intracellular ICAM-1 that was endocytosed from the cell surface should colocalize with lectin and appear yellow (green FITC + red TxR). Cell-surface ICAM-1, which did not colocalize with lectin, should appear turquoise (blue Alexa Fluor 350 + green FITC) and intracellular ICAM-1, which does not colocalize with lectin, should be green (FITC). Tracking these different fractions and their ratios over time, it is possible to discern potential trafficking of ICAM-1 between the cell surface and internal compartments by fluorescence microscopy. The mechanism of such a transport was also tested in the presence of 3 mM amiloride (inhibited in CAM-mediated endocytosis and macropinocytosis) or 0.5  $\mu$ M wortmannin (inhibited in macropinocytosis, not CAM-mediated endocytosis).

**Microscopy Visualization and Analysis.** Cell samples were analyzed using a 40 $\times$  or 60 $\times$  PlanApo objective and the Olympus IX81 inverted 3-axe automatic fluorescence microscope (Olympus Inc., Center Valley, PA). Samples were observed by phase contrast and fluorescence using filters from Semrock (Rochester, NY) in the red channel (excitation BP360–370 nm, dichroic DM570 nm, emission BA590–800+ nm), green channel (excitation BP460–490 nm, dichroic DM505 nm, emission BA515–550 nm), or blue channel (excitation BP380–400 nm, dichroic DM410 nm, emission BA415–480 nm). Micrographs were taken using Orca-ER camera from Hamamatsu (Bridgewater, NJ) and SlideBook 4.2 software from Intelligent Imaging Innovations (Denver, CO). Images were analyzed using Image-Pro 6.3 from Media Cybernetics Inc. (Bethesda, MD). Macros programmed for image analysis automatically quantify total fluorescence over background, number of objects  $\sim$ 100–300 nm, and colocalization of objects labeled with different fluorophores.<sup>14,15,41,42</sup>

**Statistical Analysis.** Data were calculated as mean  $\pm$  standard error of the mean (SEM). For each experimental condition the number of independent coverslip samples was  $\geq$ 4. Significance was determined using the Student's unpaired *t*-test assuming a *p*-value of 0.05.

## RESULTS

### Degree of Uptake of Monomeric vs Multimeric ICAM-1 Ligands.

**Ligands.** A well characterized monoclonal antibody to human ICAM-1 (R6.5)<sup>43,44</sup> was used as a model ligand capable of specific binding to ICAM-1 on human endothelial cells. To provide monomeric vs multimeric binding, the antibody was used either as a naked molecule in solution or as multiple copies coated on the surface of polymer nanoparticles (see the experimental section for details), both of which have been extensively characterized.<sup>14–20</sup> As previously demonstrated,<sup>14,15,20,38,42</sup> these two ICAM-1 binding entities showed specificity against ICAM-1 expressed on activated endothelial cells: 174 NCs/cell after a 60 min incubation (90-fold over nonspecific IgG NCs) and  $3.8 \times 10^8$  fluorescence units (38-fold over IgG).

Incubation of human endothelial cells with anti-ICAM vs anti-ICAM NCs was conducted in a pulse-chase manner (see experimental section) to track endocytosis without concomitant binding taking place. We used an established technique that allows differential visualization of cell-surface-bound (yellow color in Figure 1A) vs internalized (green color) ligands by fluorescence microscopy.<sup>14–18,45</sup> This allowed us to observe a significantly high uptake of multimeric anti-ICAM NCs, as expected:  $\sim$ 90% of total cell-associated carriers by 1 h (Figure 1B). Negligible binding of control nonspecific IgG or

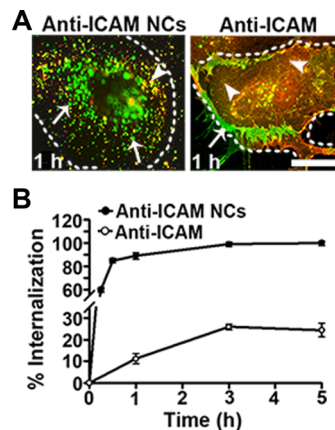


**Figure 1.** Comparative uptake of monomeric vs multimeric ICAM-1 ligands. (A) TNF- $\alpha$ -activated HUVECs were incubated with monomeric vs multimeric ligands (anti-ICAM vs anti-ICAM NCs) for 30 min to enable binding to cell-surface ICAM-1 (pulse period). After washing unbound materials, cells were incubated at 37 °C for various time intervals to allow subsequent uptake (chase period). Samples were then fixed and cell-surface vs internalized ligands were differentially stained (see experimental section for details) so that the former appear yellow (green + red; arrowheads) while internalized materials appear green (arrows). Dashed lines mark the cell borders. Scale bar, 10  $\mu$ m. (B) Internalization was calculated automatically by fluorescence image analysis as the percentage of internalized ligands relative to the total amount of cell-associated ligands. Percent internalization values are means  $\pm$  SEM. Where not visible, SEM bars are masked by the value symbol.

IgG NCs (described above) rendered uptake undetectable. Internalization of monomeric anti-ICAM was markedly lower at this time:  $\sim$ 10% of total cell-associated antibodies (9-fold below the level of uptake of anti-ICAM NCs), as observed previously.<sup>20</sup> Yet, uptake of anti-ICAM increased  $\sim$ 2.5-fold by 3 h, decreasing the difference against anti-ICAM NCs to 3.5-fold. Anti-ICAM reached a maximal uptake level of 25% vs 100% for anti-ICAM NCs. Hence, although to a much lower extent than anti-ICAM NCs, internalized anti-ICAM still represented a considerable fraction with regard to the total amount of antibodies that initially bound to cells.

Interestingly, examination of the distribution of internalized anti-ICAM vs anti-ICAM NCs (Figure 1A) revealed that internalized anti-ICAM localized to the cell periphery, whereas anti-ICAM NCs resided in the perinuclear region of the cell, which has been previously shown to correspond to lysosomal compartments<sup>42</sup> and will be subsequently verified here. This may be due to a differential mechanism of uptake between the monomeric and multimeric ligands or a difference in the route of intracellular trafficking.

**Mechanism of Uptake of Monomeric vs Multimeric ICAM-1 Ligands.** Hence, we next examined the mechanism responsible for uptake of monomeric anti-ICAM by endothelial cells against that of multimeric anti-ICAM NCs, previously identified as clathrin- and caveolae-independent CAM-mediated endocytosis.<sup>14,16</sup>

As shown in Figure 2A, internalization of both anti-ICAM and anti-ICAM NCs was driven by active means since incubation at 4 °C abolished this phenomenon: at this temperature uptake was lowered to 7% for anti-ICAM and 1% for anti-ICAM NCs (30 min), which is consistent with an endocytic event. However, given the different kinetics, maximal uptake levels, and subcellular distribution observed above for internalization of

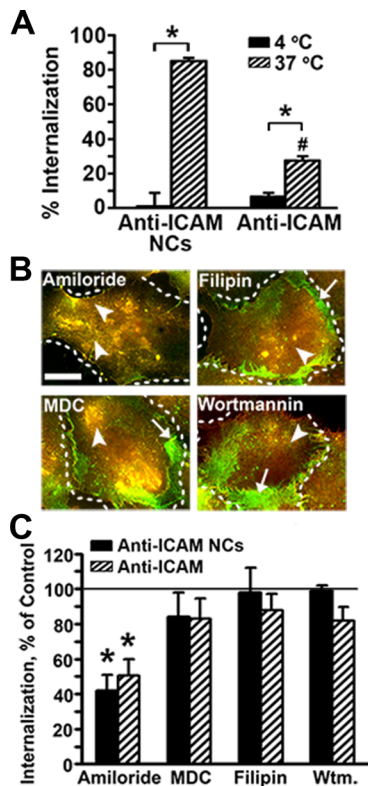


**Figure 2.** Mechanism of uptake of monomeric vs multimeric ICAM-1 ligands. (A) TNF- $\alpha$ -activated HUVECs were incubated with monomeric anti-ICAM or multimeric anti-ICAM NCs for 30 min at 4 °C or at 37 °C. Cell-surface vs internalized ligands were imaged and quantified as described in Figure 1. Percent internalization values are means  $\pm$  SEM \*:  $p < 0.05$  comparing 4 °C vs 37 °C. #:  $p < 0.05$  comparing anti-ICAM vs anti-ICAM NCs. (B) TNF- $\alpha$ -activated HUVECs were incubated with anti-ICAM or anti-ICAM NCs for 1 h at 37 °C in the absence (Control) or presence of inhibitors of CAM endocytosis and macropinocytosis (amiloride), macropinocytosis alone (wortmannin (wtm.)), clathrin-coated pits (monodansylcadaverine (MDC)), or caveoli (filipin). Cell-surface vs internalized ligands were stained as indicated in Figure 1. Dashed lines mark the cell borders. Scale bar, 10  $\mu$ m. (C) The percent internalization was calculated as in Figure 1 and normalized to that in Control cells. \*:  $p < 0.05$  comparing inhibitors to the control.

monomeric vs multimeric ICAM-1 ligands, it would seem plausible that uptake of these counterparts operates via different mechanisms.

Surprisingly, this was not the case (Figure 2B). Just as anti-ICAM NCs, uptake of anti-ICAM was not affected by MDC (83% of control) or filipin (88% of control), which are inhibitors of clathrin- and caveolin-mediated pathways, respectively. In addition, amiloride, an inhibitor of CAM-mediated endocytosis and macropinocytosis, markedly reduced uptake of anti-ICAM, anti to a similar extent to that inhibition of ICAM NCs (~50% by 1 h). Wortmannin, an inhibitor of phosphoinositide 3-kinase (PI3K) associated with macropinocytosis but not CAM-mediated endocytosis, did not significantly alter the degree of uptake of anti-ICAM (83% of control). This was also the case for anti-ICAM NCs (99% of control). Therefore, uptake of both monomeric and multimeric ICAM-1 ligands appears to be regulated by CAM-mediated endocytosis, despite the differences noted above.

#### Lysosomal Trafficking and Degradation of Monomeric vs Multimeric ICAM-1 Ligands.

Since monomeric

anti-ICAM and multimeric anti-ICAM NCs seem to undergo the same mechanism of endocytosis, it is possible that their different levels of uptake may reflect different intracellular trafficking. Differential distribution of these ligands at the cell periphery vs the perinuclear region after endocytosis, as observed above, seems to support this hypothesis. Hence, to examine this aspect in more detail, we examined the potential colocalization of intracellular anti-ICAM to lysosomal compartments characterized by the presence of LAMP-1 (Figure 3A)

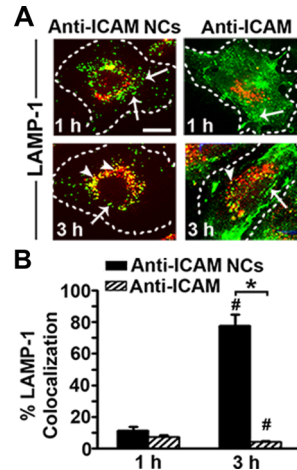


**Figure 3.** Lysosomal trafficking of monomeric vs multimeric ICAM-1 ligands. (A) TNF- $\alpha$ -activated HUVECs were incubated with green-fluorescent anti-ICAM or anti-ICAM NCs for a 30 min pulse, washed, incubated for up to 1 or 3 h at 37 °C, then fixed and permeabilized. Lysosomes were labeled with TxR anti-LAMP-1 (red). Yellow color represents green anti-ICAM or anti-ICAM NCs localized to the red-labeled lysosomes, marked by arrowheads. Arrows represent anti-ICAM or anti-ICAM NCs, which do not colocalize with anti-LAMP-1. Dashed lines mark the cell borders. Scale bar, 10  $\mu$ m. (B) The percent colocalization with LAMP-1 with respect to the total cell-associated anti-ICAM or anti-ICAM NCs was quantified by fluorescence image analysis. Data are means  $\pm$  SEM. \*:  $p < 0.05$  comparing anti-ICAM vs anti-ICAM NCs. #:  $p < 0.05$  comparing 1 h vs 3 h.

since this represents a predominant destination for anti-ICAM NCs.<sup>39,42</sup> Indeed, 78% of all cell-associated anti-ICAM NCs colocalized with LAMP-1-positive compartments by 3 h (Figure 3B). In contrast, minimal lysosomal colocalization was observed for anti-ICAM: <7.5% within this time frame.

We must note that, in this experiment, fluorescent tracking of anti-ICAM NCs focuses on the polymeric component (fluorescent polystyrene), which is nondegradable. Instead, lysosomal colocalization of anti-ICAM may go unnoticed if the antibody was subjected to proteolytic degradation in lysosomes. Therefore, we examined potential changes over time in the level of immunodetectable anti-ICAM associated with cells, which would be indicative of its degradation (Figure 4). In agreement with the lack of lysosomal colocalization observed above, only 15% of cell-associated anti-ICAM seemed to disappear over a period of 5 h. This was in contrast to anti-ICAM NCs. Immunodetection of anti-ICAM on the surface of green-fluorescent carriers using a red-labeled secondary antibody (which renders yellow color only when the antibody coat is present on green particles; Figure 4A), showed considerable degradation of anti-ICAM on carriers over time: from 8% at 1 h, to 67% at 3 h, and 85% by 5 h (Figure 4B), in agreement with their lysosomal trafficking (Figure 3B).

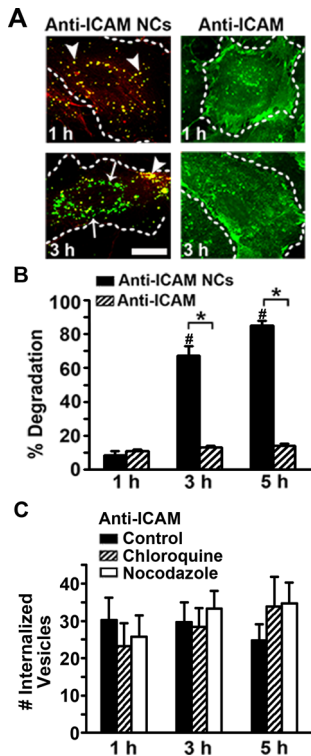


**Figure 4.** Degradation of monomeric vs multimeric ICAM-1 ligands. (A) TNF- $\alpha$ -activated HUVECs were treated with green-fluorescent anti-ICAM or anti-ICAM NCs for a 30 min pulse to allow only binding, then washed and incubated for up to 1, 3, or 5 h at 37 °C to allow uptake. Cells were then fixed and permeabilized. For nanocarriers, permeabilized cells were immunolabeled with TxR-goat antimouse IgG, which binds nondegraded anti-ICAM on the carrier surface to produce yellow, double-labeled particles (arrowheads). The green, single-labeled fraction represents nanocarriers with a nonimmunodetectable (herein called degraded) antibody coat (arrows). In the case of anti-ICAM, nondegraded antibody associated with cells is shown in green, which should diminish over time if there was degradation. Dashed lines mark the cell borders. Scale bar, 10  $\mu$ m. (B) Percentage of nanocarriers, which lack immunodetectable anti-ICAM and percent of anti-ICAM compared to the initial anti-ICAM fluorescence at 30 min. (C) Number of intracellular vesicles containing anti-ICAM after incubation in control cell medium vs medium containing chloroquine or nocodazole during the chase period. Data are means  $\pm$  SEM. \*:  $p < 0.05$  comparing anti-ICAM vs anti-ICAM NCs. #:  $p < 0.05$  with respect to degradation after 30 min.

To further ensure that degradation of monomeric anti-ICAM did not go unnoticed, similar experiments were performed in the presence of chloroquine, an agent that inhibits acidification and, hence, lysosomal degradation,<sup>42</sup> or in the presence of nocodazole, an agent that disrupts lysosomal trafficking by altering the microtubular network.<sup>42</sup> Uptake was not affected in the presence of chloroquine or nocodazole ( $85 \pm 15\%$  and  $120 \pm 15\%$  of control uptake at 3 h; not shown). Moreover, neither agent decreased degradation of anti-ICAM any further (10% and 15% degradation observed for chloroquine and nocodazole vs 11% for the control at 1 h; not shown). In addition, if there was any trafficking of anti-ICAM to lysosomes, it would be expected that inhibition of lysosomal degradation would increase the number of anti-ICAM vesicles that remain visible over time. However, as shown in Figure 4C, this parameter remained nearly constant (~25–35 vesicles/cell) over 5 h and similar to the control.

**Uptake and Intracellular Trafficking of Multimeric Anti-ICAM Conjugates.** To ascertain whether the differential trafficking of anti-ICAM NCs vs monomeric anti-ICAM was due to chemical/physical factors associated with the polymer particle, we examined another multimeric ligand: biotinylated anti-ICAM conjugated with streptavidin. This model differed from anti-ICAM NCs in size (320 nm vs 150 nm in diameter) and charge (−4 vs −30 mV), yet it similarly represents a multivalent entity. Cells incubated with anti-ICAM conjugates from 30 min to 5 h showed 94–99% colocalization between the streptavidin and anti-ICAM counterparts, verifying that conjugate components remain linked throughout this time (not shown). Binding of anti-ICAM conjugates to cells was specific: 261 objects/cell at 30 min, which was reduced by 65% in the presence of anti-ICAM competitor (data not shown). Importantly, over time, anti-ICAM conjugates displayed a significant and increasing perinuclear localization (up to 77% at 5 h) and uptake (up to 72% at 5 h) as in the case of anti-ICAM NCs (compare Figure 5A vs Figures 1A,B and 6C), suggesting that this is a general property of multimeric ICAM-1 ligands.

However, when we examined colocalization of anti-ICAM conjugates with LAMP-1-labeled lysosomes (Figure 5B), we found poor colocalization (e.g., 15% at 5 h). Since LAMP-1 labeling requires permeabilization, this result may be due to lysosomal degradation of anti-ICAM conjugates and leaching of the fluorophore after permeabilization. Indeed, upon quantification of the total cell-associated fluorescence of anti-ICAM and streptavidin components of the conjugate over time (Figure 5C), we found significant decay for both (53% and 58% degradation at 5 h, respectively), suggesting degradation. In addition, the number of perinuclear vesicles containing conjugates significantly decreased with permeabilization (13 vs 33 vesicles at 1 h for permeabilized vs nonpermeabilized cells; Figure 5B). This result implied escape of the fluorophore from these compartments, also indicative of conjugate degradation. Hence, to avoid permeabilization that precludes visualizing conjugates within degradative compartments, we prelabeled lysosomes using TxR dextran as described.<sup>42</sup> To ensure consistency between the two methods, we revealed a similar quantity of intracellular vesicles labeled by anti-LAMP-1 antibodies and dextran (~65–70 vesicles/cell). Importantly, significant and increasing colocalization of anti-ICAM conjugates with dextran-labeled lysosomes was observed (e.g., 65% at 5 h), which was similar to anti-ICAM NCs and different from monomeric anti-ICAM (Figure 3).

**Routing of Monomeric vs Multimeric ICAM-1 Ligands to the Cell Periphery.** The aforementioned results revealed that monomeric anti-ICAM, not multimeric counterparts, avoided lysosomal compartments and the associated degradation (Figures 3 and 4). Also, internalized monomeric anti-ICAM, not multimeric forms, had been observed to localize to the cell periphery (Figures 1A and 5A). This clearly indicates that, although exploiting the same endocytic pathway into cells, monomeric anti-ICAM follows a different intracellular routing from multimeric anti-ICAM NCs.

To complement these studies, we analyzed this differential subcellular distribution (Figure 6A). In accord with lysosomal trafficking and degradation, the fraction of internalized anti-ICAM NCs detected at the cell periphery decreased with time (from ~40% at 30 min to ~15% at 5 h; Figure 6B), while the fraction located at the perinuclear region increased (from ~25% at 30 min to ~85% at 5 h; Figure 6C), similar to anti-ICAM conjugates (Figure 5A). In contrast, in agreement with its lack of lysosomal routing and degradation, the trafficking of

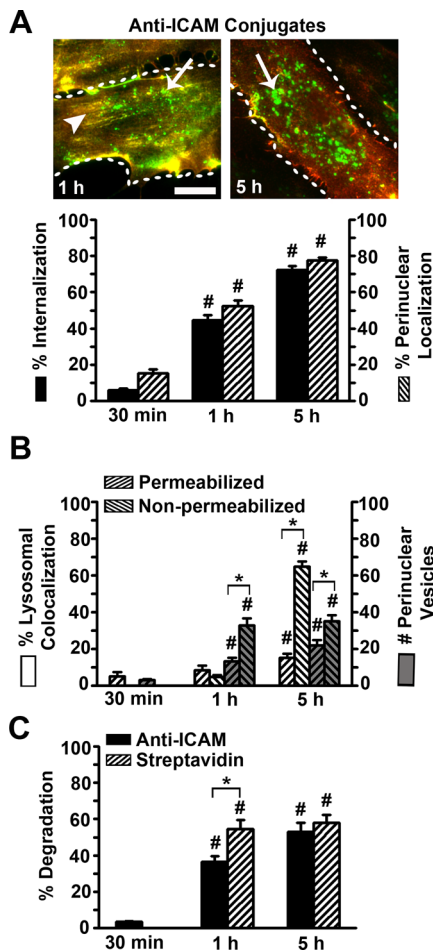


**Figure 5.** Uptake and intracellular trafficking of multimeric anti-ICAM conjugates. (A) TNF- $\alpha$ -activated HUVECs were treated with green-fluorescent anti-ICAM conjugates for a 30 min pulse to permit only binding, then washed and incubated for up to 1, 3, or 5 h at 37 °C to allow uptake. Cells were then fixed, and surface-bound conjugates were immunolabeled with TxR-goat antimouse IgG (yellow; arrowheads). The green, single-labeled fraction represents internalized counterparts (arrows). Dashed lines mark the cell borders. Scale bar, 10  $\mu$ m. The percentage of internalized conjugates relative to the total cell-associated fraction and the percentage of internalized, perinuclear conjugates relative to the total internalized fraction were quantified by fluorescence microscopy. (B) Percentage of green-labeled anti-ICAM conjugates colocalized with red lysosomes labeled by two methods: (1) permeabilization and staining with TxR anti-LAMP-1 vs prelabeling with TxR dextran prior to incubation with conjugates (nonpermeabilized cells).<sup>42</sup> The number of perinuclear vesicles containing conjugates was also quantified by fluorescence microscopy. (C) Percentage of anti-ICAM or streptavidin compared to the initial anti-ICAM fluorescence at 30 min. Data are means  $\pm$  SEM. #:  $p < 0.05$  with respect to data at the initial time point. \*:  $p < 0.05$  comparing permeabilized to nonpermeabilized cells (B) or anti-ICAM vs streptavidin (C).

anti-ICAM to the perinuclear region of cells remained very low over time (~8% at 30 min and ~12% at 5 h; Figure 6C), while it remained stably located at the cell periphery (~68% at 30 min and ~77% at 5 h; Figure 6B).

**Recycling Routing of Monomeric vs Multimeric ICAM-1 Ligands.** We next tested whether the peripheral localization observed for monomeric anti-ICAM may be associated with recycling from endocytic compartments to the plasma membrane. For this purpose, we comparatively examined the colocalization

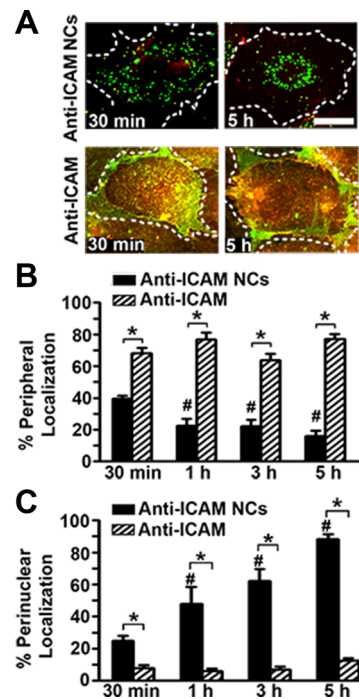


**Figure 6.** Peripheral and perinuclear localization of monomeric vs multimeric ICAM-1 ligands. (A) TNF- $\alpha$ -activated HUVECs were incubated with anti-ICAM or anti-ICAM NCs for a 30 min pulse to allow only binding, then washed and incubated for up to 30 min, 1, 3, or 5 h at 37 °C to allow uptake. Cells were fixed and immunostained as described in Figure 1 to differentially label surface-bound (yellow) vs internalized (green) fractions. Dashed lines mark the cell borders. Scale bar, 10  $\mu$ m. (B) Fluorescence image analysis was used to quantify the percentage of internalized anti-ICAM or anti-ICAM NCs localized to the cell periphery (within ~5  $\mu$ m from the cell border) or (C) perinuclear region (within ~5  $\mu$ m from the nucleus) relative to the total internalized fraction. Values are means  $\pm$  SEM. \*:  $p < 0.05$  comparing anti-ICAM vs anti-ICAM NCs. #:  $p < 0.05$  with respect to percent localization after the pulse (30 min).

of anti-ICAM vs anti-ICAM NCs (green in Figure 7A) with Rab11a (red). This marker belongs to the small GTPase superfamily of proteins and has been well established for its role in the recycling of various ligands and/or their receptors, including transferrin, transferrin receptor, E-cadherin, LFA-1, GLUT4, etc.<sup>35,46–50</sup> Surprisingly, fluorescence microscopy revealed that both anti-ICAM and anti-ICAM NCs colocalized significantly with Rab11a-positive compartments after internalization (yellow color): ~75%–85% in the case of anti-ICAM and ~55%–60% for anti-ICAM NCs within the first hour (Figure 7B). However, localization of anti-ICAM NCs with Rab11a decayed to 23% by 3 h and 13% by 5 h. This was not the case for anti-ICAM, a substantial fraction of which remained within this compartment even after 5 h (75%).

Therefore, it appears that both anti-ICAM and anti-ICAM NCs enter cells via the same pathway and initially traffic to a similar membrane-proximal intracellular compartment, yet anti-ICAM recycles back to the plasmalemma, while anti-ICAM NCs deviate to lysosomes. Supporting this, tracking the cell-surface vs intracellular distribution of monomeric anti-ICAM over time revealed that, while the total cell-associated fraction remained constant (~90% of the original value at 30 min), the intracellular fraction cycled: this fraction decreased by 65% at 1 h, then increased to 83% of the original value by 3 h (Figure 8). This result could be visualized by fluorescence microscopy in

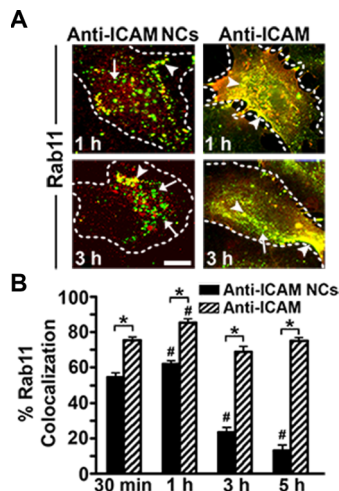


**Figure 7.** Colocalization of monomeric vs multimeric ICAM-1 ligands with recycling compartments. (A) TNF- $\alpha$ -activated HUVECs were incubated with green fluorescent anti-ICAM for a 30 min pulse to allow only binding, then washed and incubated for up to 30 min, 1, 3, or 5 h at 37 °C to allow uptake. Cells were then washed, fixed, and permeabilized. Recycling compartments were labeled with antibodies to Rab11a and a TxR secondary antibody. Arrowheads denote green anti-ICAM or anti-ICAM NCs localized to red-labeled compartments (yellow color), and arrows represent noncolocalized counterparts (green color). Dashed lines mark the cell borders. Scale bar, 10  $\mu$ m. (B) The percent Rab11a colocalization with respect to total cell-associated anti-ICAM or anti-ICAM NCs was quantified by fluorescence image analysis. Data are means  $\pm$  SEM. \*:  $p$  < 0.05 comparing anti-ICAM vs anti-ICAM NCs. #:  $p$  < 0.05 comparing Rab11a colocalization after the pulse (30 min).

that the internalized “green” fraction of anti-ICAM at the cell periphery nearly disappeared (compare 30 min vs 1 h), then reaccumulated (compare 1 h vs 3 h).

**Endocytic Recycling of Endothelial ICAM-1 in the Absence of Ligands.** In a previous study it was observed that internalized multimeric anti-ICAM NCs trafficked to early endosomal compartments, from which the receptor, ICAM-1, recycled back to the cell surface, while carriers trafficked to lysosomes.<sup>15</sup> Since it is known that Rab11a recycling compartments can arise from early endosomes, it seems that recycling of monomeric anti-ICAM observed in this study may simply be following the itinerary of its receptor after uptake. If this is the case, the question remains whether anti-ICAM induces endocytosis and recycling upon binding to ICAM-1, or whether ICAM-1 is constitutively endocytosed and recycled in activated endothelial cells whereby anti-ICAM simply remains bound to (and follows) its receptor.

To assess the latter possibility, we tracked the cellular location of ICAM-1 in the absence of ligands (Figure 9A). We first labeled the cell surface using red-fluorescent lectin, which binds to glycoproteins on the plasma membrane, hence, allowing us to track intracellular compartments that may originate from the cell surface as red punctate structures (asterisks). At various times after labeling the plasmalemma, surface-located ICAM-1 was immunostained in blue and total (surface + intracellular) ICAM-1 was additionally immunostained in green (see experimental section for details). As expected, this protocol revealed colocalization of cell surface ICAM-1 (blue + green) with lectin (red), which appeared as triple labeled regions (white; denoted by arrowheads). The presence of white regions decreased with time (compare 30 min or 1 h with 5 h),

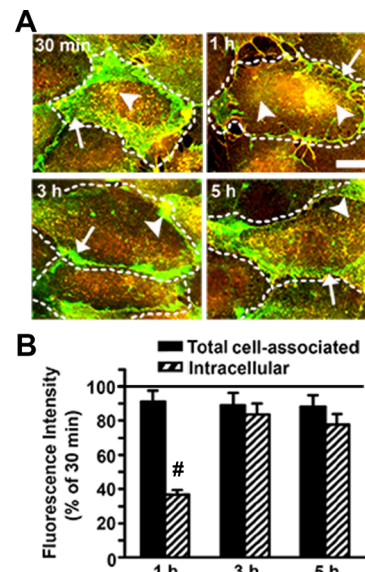


**Figure 8.** Recycling of monomeric anti-ICAM. (A) TNF- $\alpha$ -activated HUVECs were incubated with monomeric anti-ICAM for 30 min to enable binding to cell-surface ICAM-1 (pulse period), washed to remove unbound materials, and incubated for various time intervals at 37 °C to allow subsequent uptake and/or recycling to the cell surface (chase period). Samples were then fixed and cell-surface vs internalized ligands were differentially stained yellow (green + red; arrowheads) and green (arrows), respectively. Dashed lines mark the cell borders. Scale bar, 10  $\mu$ m. (B) Fluorescence intensity of total cell-associated and intracellular anti-ICAM was quantified by fluorescence image analysis and expressed as a fraction of the respective amount after the pulse (30 min; solid line). Values are means  $\pm$  SEM. #:  $p$  < 0.05 with respect to the fluorescence intensity at 30 min.

as expected if ICAM-1 was endocytosed. Verifying this, intracellular ICAM-1 (green with no blue label) could be found to colocalize with punctate lectin-containing compartments (red), indicating that this pool had been endocytosed from the plasmalemma (yellow; denoted by arrows). This fraction represented ~16% of total ICAM-1 (Figure 9B). Also, we found a fraction of intracellular ICAM-1 (green) that did not colocalize with lectin (red), which may originate from the biosynthetic route. Therefore, it appears that indeed surface-expressed ICAM-1 is endocytosed in the absence of ligands.

Interestingly, with time, there was an increase in the fraction of lectin that distributed to the perinuclear region of the cell (from 36% at 30 min to 75% at 5 h; Figure 9C), and this coincided with a decrease in the colocalization of ICAM-1 and lectin (from 16% at 30 min to 6% by 5 h). This would be in agreement with endocytic transport of ICAM-1 away from perinuclear compartments, just as observed when studying endocytosis of anti-ICAM (Figure 6).

To verify this, we examined the fraction and location of intracellular ICAM-1 in the absence of ligands (sham), using cells that were previously treated with cycloheximide to minimize the presence of intracellular ICAM-1 originating from the biosynthetic route (Figure 10). These cells were fixed and cell surface vs intracellular ICAM-1 were differentially immunostained (yellow and green, respectively; see experimental section for details). This revealed the presence of intracellular ICAM-1 at the cell periphery (Figure 10A), representing ~26% of total ICAM-1 (Figure 10B). This is comparable to the location and fraction of anti-ICAM (29%) that is endocytosed by cells upon incubation with this ligand (Figure 1B). Amiloride reduced the

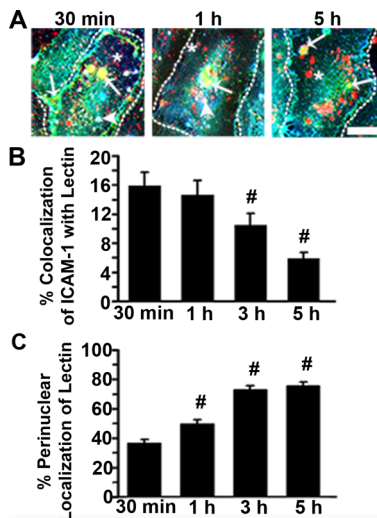


**Figure 9.** ICAM-1 internalization in the absence of ligand binding. (A) TNF- $\alpha$ -activated HUVECs were incubated at 37 °C continuously for different time intervals with TxR tomato lectin (red) to label the cell surface and allow potential endocytosis. Cells were then fixed and immunostained to visualize surface-bound ICAM-1 in blue, followed by permeabilization and immunostaining of total ICAM-1 (surface and internal) in green. Colocalization of surface ICAM-1 with lectin appears in white (arrowheads). Colocalization of intracellular ICAM-1 with lectin (therefore, originating from the plasmalemma) appears in yellow (arrows). Asterisks indicate punctate lectin-containing compartments (red; generated from endocytosis), which do not colocalize with ICAM-1. Dashed lines mark the cell borders. Scale bar, 10  $\mu$ m. (B) The extent of colocalization of ICAM-1 and lectin was quantified by fluorescence image analysis. (C) The percentage of lectin localized to the perinuclear region (within ~5  $\mu$ m from the nucleus) relative to the total amount of cell-associated lectin is also shown. Data are means  $\pm$  SEM. #:  $p < 0.05$  against values at the initial time point (30 min).

fraction of intracellular ICAM-1 by 68% (Figure 10C), similar to the inhibition observed with regard to uptake of anti-ICAM shown in Figure 2B. Also, in parallel to results obtained in the presence of these ligands, wortmannin did not reduce the level of intracellular ICAM-1 in the absence of ligands.

This set of results indicates that ICAM-1 is endocytosed from the endothelial plasmalemma in the absence of ligands and is routed through similar peripheral compartments, via CAM-mediated endocytosis.

## ■ DISCUSSION

Many cell surface receptors undergo different endocytic outcomes when bound to ligands, e.g., monomeric vs multimeric counterparts, compared to their unbound state. Yet, this is still a rather unexplored phenomenon, particularly in cases where natural ligands of a receptor represent multimeric engagement entities. The present study has examined these aspects in the case of endothelial ICAM-1, using monomeric anti-ICAM vs multimeric anti-ICAM NCs and conjugates as representative ligands. Although previous investigations had deemed monomeric anti-ICAM unable to enter cells as multimeric anti-ICAM counterparts (NCs and conjugates) do,<sup>14,20</sup> to our surprise, a closer examination revealed appreciable uptake via a similar mechanism, CAM-mediated endocytosis. Lower apparent or steady-state levels of endocytosis of monomeric anti-ICAM resulted from a distinct intracellular itinerary. At initial time points, both anti-ICAM and anti-ICAM NCs localized to Rab11a compartments at the cell periphery. Yet, with time, anti-ICAM

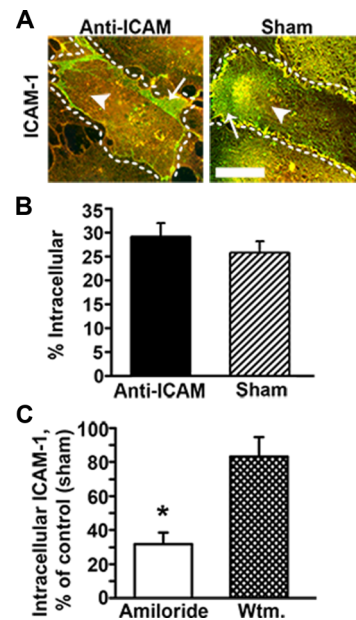


**Figure 10.** Presence of intracellular ICAM-1 in the absence of ligand binding. (A) TNF- $\alpha$ -activated HUVECs were incubated for 1 h at 37 °C with anti-ICAM, for ligand-induced uptake. Alternatively (sham), cells were treated with cyclohexamide (to minimize intracellular ICAM-1 arising from *de novo* synthesis) and fixed before being incubated with anti-ICAM, so that there is no ligand-induced uptake. In both cases, samples were then incubated with a TxR-secondary antibody to label ICAM-1 at the cell surface, followed by permeabilization and staining of total ICAM-1 (surface + intracellular) with anti-ICAM and FITC-secondary antibody. This labels cell-surface ICAM-1 in yellow (red + green; arrowheads) vs intracellular ICAM-1, which appears green only (arrows). Dashed lines mark the cell borders. Scale bar, 10  $\mu$ m. (B) Images were scored by fluorescence analysis to quantify the percentage of intracellular ICAM-1 with respect to the total pool of cell-associated ICAM-1. (C) A similar analysis was performed comparing sham cells from (A,B) control to sham cells treated with an inhibitor of CAM-endocytosis and macropinocytosis (amiloride) or an inhibitor of macropinocytosis only (wortmannin; wtm). Data are means  $\pm$  SEM and represent percent intracellular ICAM-1. \*:  $p < 0.05$  against control (sham) values.

NCs and conjugates trafficked to perinuclear lysosomes with significant degradation of the antibody counterpart (as previously reported<sup>42</sup>), while monomeric anti-ICAM remained localized to Rab11a-compartments with little degradation and recycled back to the plasma membrane. Similar trafficking was found for ICAM-1 in the absence of ligand binding, suggesting that this molecule recycles between the plasmalemma and an endosomal-like subplasmalemma compartment. Hence, contrary to anti-ICAM NCs and conjugates that follow an endolysosomal pathway, anti-ICAM simply follows the route of the receptor.

These results demonstrate a clearly differential endocytic fate for monomeric vs multimeric ligands against ICAM-1. The pattern observed for this cell surface marker held similarities and differences as compared to other receptors. For instance, greater uptake of multimeric anti-ICAM NCs with respect to monomeric anti-ICAM contrasted observations of slower internalization of an oligomer composed of ten transferrin molecules vs monomeric transferrin.<sup>7</sup> Yet, greater intracellular retention of anti-ICAM NCs relative to anti-ICAM was somewhat similar to longer intracellular retention of transferrin oligomers vs monomeric transferrin.<sup>7</sup> Nevertheless, multimeric ligands in these two cases resided in different sites, i.e., lysosomes

for multimeric ICAM-1 ligands as opposed to pericentriolar recycling compartments for multimeric transferrin counterparts.<sup>7</sup> Another example is that of monomeric folate-drug conjugates vs multivalent folate-decorated carriers.<sup>8</sup> Analogous to ICAM-1, multivalent folate carriers trafficked to lysosomes, whereas monomeric folate conjugates followed a recycling route to the plasma membrane.<sup>8</sup> However, distinct from ICAM-1, multivalent folate carriers followed the route of the natural ligand (folate)-receptor pair,<sup>8</sup> whereas monomeric anti-ICAM followed the recycling route of unbound ICAM-1. Antibody receptors have also shown different patterns of endocytic routing for different ligands, e.g., binding of an artificial monovalent ligand of macrophage Fc receptor (a modified Fab) resulted in recycling to the cell membrane, whereas a polyvalent immunoglobulin G complex triggered lysosomal trafficking and degradation.<sup>11,12</sup> However, no difference in the final intracellular destination was found between these divalent and polyvalent Fc receptor ligands, while this was not the case for ICAM-1 (anti-ICAM shown here is divalent).

The differences observed between monomeric and multimeric anti-ICAM ligands are not due to physicochemical characteristics of the polymer particle in the case of anti-ICAM NCs, since a similar uptake, perinuclear distribution, lysosomal colocalization, and degradation was found for multivalent anti-ICAM conjugates formed by cross-linking biotinylated anti-ICAM with streptavidin. It is likely that different physicochemical properties of the carrier may further impact the intracellular behavior. Yet, the fact that multimeric ICAM-1-targeted entities with diverse composition and valency (anti-ICAM-coated PLGA particles, DNA-built dendrimers, liposomes, etc.) behave similarly in terms of intracellular trafficking<sup>27,51,52</sup> supports that this is a general feature of multimeric vs monomeric targeting to ICAM-1. However, it is possible that intracellular trafficking to other receptors and pathways may be more sensitive to variations of the carrier formulation.

Importantly, our results indicate that intracellular trafficking of anti-ICAM reflects a pathway by which endothelial ICAM-1 seems to recycle between the cell surface and a subplasmalemma compartment in the absence of ligand binding, which was previously overlooked. This was supported by the fact that, in the absence of *de novo* protein synthesis or ICAM-1 ligands, ICAM-1 expressed on the cell surface was internalized, as observed by tracking the endothelial plasmalemma after lectin-labeling. Following uptake, ICAM-1 diverged from the perinuclear distribution of lectin-positive internalized compartments. This, along with the lack of significant disappearance (reflective of degradation) of immunodetectable ICAM-1 with time and reappearance of this molecule at the cell surface suggest that endocytosed ICAM-1 is not destined for lysosomal degradation but recycling. This may explain why endocytosis of monomeric anti-ICAM had been overlooked in the past.<sup>14,20</sup>

Given that the outcome and kinetics for all these events were similar upon ICAM-1 engagement by monomeric anti-ICAM, it is possible that this ligand does not induce endocytosis and rather passively follows the route of the receptor to which it is bound. Multimeric anti-ICAM NCs are also internalized via CAM-mediated endocytosis and localized at early time points to similar Rab11a compartments. However, from here this ligand did not follow subsequent recycling but lysosomal transport, as previously shown.<sup>15,21</sup> Hence, multimeric engagement of the receptor may not provide the signal for CAM-endocytosis as previously believed,<sup>14,20</sup> but rather the signal to deviate the subsequent intracellular trafficking from the "constitutive"

recycling route. In fact, a previous study had shown that, although anti-ICAM NCs traffic to endolysosomal compartments within cells, a significant fraction of ICAM-1 cointernalized with such carriers also recycles back to the plasmalemma.<sup>15</sup> The fact that higher uptake is observed for anti-ICAM NCs and conjugates vs anti-ICAM may be due not to a greater endocytic efficiency but to cumulative retention of endocytosed carriers within the cell. Hence, anti-ICAM recycling, which leads to lower intracellular accumulation, would be misinterpreted as a lower degree of endocytosis.

From a biological standpoint, ICAM-1 uptake and recycling by endothelial cells in the absence of ligands is a new finding whose biological significance remains to be elucidated. However, recycling of membrane determinants is a common process, broadly involved in numerous cellular processes, such as cell-cell adhesion, migration, polarization, differentiation, and signaling.<sup>1,46,48,53</sup> In fact, in antigen presenting cells (APCs), ICAM-1 has been observed to undergo uptake and recycling at sites of T-cell contact, which was mediated by an amiloride-sensitive pathway,<sup>37</sup> analogous to CAM endocytosis in endothelial cells. This uptake and recycling seemed to provide a continuous redistribution of ICAM-1 on the APC surface, which helped maintain the dynamic contact with T-cells and strengthen cell-cell signaling.<sup>37</sup> In addition, platelet-endothelial cell adhesion molecule 1 (PECAM-1), a surface molecule structurally and functionally related to ICAM-1, and also associated with CAM endocytosis, has been shown to undergo constant recycling through specialized submembrane compartments of endothelial cells, to guide transmigration of leukocytes across the endothelium.<sup>54</sup> It is possible that CAM-mediated endocytosis of ICAM-1 represents an analogous phenomenon. Indeed, ICAM-1 also contributes to extravasation of leukocytes, where ICAM-1 continuously redistributes on the endothelial surface toward the migrating fronts of leukocyte contacts.<sup>55</sup>

From a translational perspective, the findings of this study significantly extend previous knowledge on the potential for targeted drug delivery via ICAM-1. As indicated above, ICAM-1 is being explored for targeted interventions against conditions involving inflammation, immune disorders, cardiovascular disease, genetic and metabolic syndromes, etc.<sup>20–29,56–58</sup> In most of these settings, multivalent targeting to ICAM-1 has been pursued, e.g., by coupling affinity moieties to liposomes, microbubbles, polymer particles, gold nanorods, iron oxide nanoparticles, and other NC formulations.<sup>20–29,56–58</sup> By providing endocytosis and intraendothelial trafficking, said multimeric ICAM-1-targeting strategies are valuable for intracellular drug delivery to cope with these maladies. For instance, lysosomal transport of multimeric ICAM-1-targeted carriers is ideal for delivery of lysosomal enzyme replacement therapies necessary to treat genetic deficiencies of these enzymes (i.e., lysosomal storage disorders).<sup>9,21,22,39,59</sup> However, lysosomal trafficking is expected to result in premature degradation and/or entrapment of most other therapeutic agents.<sup>15,42</sup> Therefore, delivery by conjugation to monomeric ICAM-1-targeting ligands may resolve this problem by avoiding lysosomal transport while retaining the therapeutic agent within the endothelium via an uptake-recycling pathway, providing more sustained delivery. This is feasible since several ICAM-1 targeting monoclonal antibodies, their humanized counterparts, antibody fragments, and peptides have shown efficient ICAM-1 targeting and significant safety in animal models and clinical trials.<sup>9,21,57,60–63</sup>

In conclusion, the studies herein have provided insight into the differential endocytic fates associated with bound

(via monomeric vs multimeric ligands) and unbound endothelial ICAM-1. This highlights the complex regulation of endocytic events, which at present still remain elusive, particularly for nonconventional clathrin- and caveolae-independent pathways such as CAM-mediated endocytosis. Our findings reveal that this pathway may be a constitutive process in activated endothelial cells, which provides a means to maintain a subplasmalemma pool of recycling ICAM-1 molecules. This pool may allow for rapid redistribution of ICAM-1 to the cell surface, e.g., at sites of adhesion by natural ligands (primarily leukocytes). ICAM-1-trafficking does not appear to be disrupted by binding of monomeric affinity molecules but by multimeric carriers, which traffic to lysosomes. These findings pair well with the biological function of ICAM-1 and provide new avenues for therapeutic targeting to this endothelial marker. For instance, monomeric delivery vehicles directed at ICAM-1 may allow more prolonged therapy without undergoing lysosomal degradation, contrary to multimeric formulations that are more amenable for delivery into endolysosomal compartments. Hence, these newly identified features are critical to the selection and optimization of formulations that tailor particular therapeutic needs.

## AUTHOR INFORMATION

### Corresponding Author

\*Tel: 1 + 301-405-4777. Fax: 1 + 301-314-9075. E-mail: muro@umd.edu.

### Notes

The authors declare no competing financial interest.

## ACKNOWLEDGMENTS

This work was supported by a National Science Foundation Graduate Research Fellowship to R.G. (DGE-0750616) and funds awarded to S.M. by the National Institutes of Health (grant R01-HL98416) and the National Science Foundation (CBET-1402756). We thank Dr. Steven M. Jay (Bioengineering, University of Maryland College Park) for kindly sharing the particle tracking instrument (NanoSight LM10) for carrier size measurements.

## ABBREVIATIONS

APC, antigen presenting cell; BSA, bovine serum albumin; FITC, fluorescein isothiocyanate; HUVECs, human umbilical vein endothelial cells; ICAM-1, intercellular adhesion molecule-1; IgG, immunoglobulin G; LAMP-1, lysosomal-associated membrane protein 1; MDC, monodansylcadaverine; NCs, nanocarriers; PECAM-1, platelet-endothelial cell adhesion molecule-1; TxR, Texas red; TNF- $\alpha$ , tumor necrosis factor alpha; Wtm, wortmannin

## REFERENCES

- (1) Grant, B. D.; Donaldson, J. G. Pathways and mechanisms of endocytic recycling. *Nat. Rev. Mol. Cell Biol.* **2009**, *10* (9), 597–608.
- (2) Brown, V. I.; Greene, M. I. Molecular and cellular mechanisms of receptor-mediated endocytosis. *DNA Cell Biol.* **1991**, *10* (6), 399–409.
- (3) Duncan, R.; Richardson, S. C. Endocytosis and intracellular trafficking as gateways for nanomedicine delivery: opportunities and challenges. *Mol. Pharmaceutics* **2012**, *9* (9), 2380–402.
- (4) Mayor, S.; Pagano, R. E. Pathways of clathrin-independent endocytosis. *Nat. Rev. Mol. Cell Biol.* **2007**, *8* (8), 603–12.
- (5) Muro, S. Challenges in design and characterization of ligand-targeted drug delivery systems. *J. Controlled Release* **2012**, *164* (2), 125–37.
- (6) Torchilin, V. Multifunctional and stimuli-sensitive pharmaceutical nanocarriers. *Eur. J. Pharm. Biopharm.* **2009**, *71* (3), 431–44.
- (7) Marsh, E. W.; Leopold, P. L.; Jones, N. L.; Maxfield, F. R. Oligomerized transferrin receptors are selectively retained by a luminal sorting signal in a long-lived endocytic recycling compartment. *J. Cell Biol.* **1995**, *129* (6), 1509–22.
- (8) Xia, W.; Low, P. S. Folate-targeted therapies for cancer. *J. Med. Chem.* **2010**, *53* (19), 6811–24.
- (9) Papademetriou, J.; Garnacho, C.; Serrano, D.; Bhowmick, T.; Schuchman, E. H.; Muro, S. Comparative binding, endocytosis, and biodistribution of antibodies and antibody-coated carriers for targeted delivery of lysosomal enzymes to ICAM-1 versus transferrin receptor. *J. Inherited Metab. Dis.* **2013**, *36* (3), 467–77.
- (10) Oh, P.; Borgstrom, P.; Witkiewicz, H.; Li, Y.; Borgstrom, B. J.; Chrastina, A.; Iwata, K.; Zinn, K. R.; Baldwin, R.; Testa, J. E.; Schnitzer, J. E. Live dynamic imaging of caveolae pumping targeted antibody rapidly and specifically across endothelium in the lung. *Nat. Biotechnol.* **2007**, *25* (3), 327–37.
- (11) Mellman, I.; Plutner, H. Internalization and degradation of macrophage Fc receptors bound to polyvalent immune complexes. *J. Cell Biol.* **1984**, *98* (4), 1170–7.
- (12) Mellman, I.; Plutner, H.; Ukkonen, P. Internalization and rapid recycling of macrophage Fc receptors tagged with monovalent antireceptor antibody: possible role of a prelysosomal compartment. *J. Cell Biol.* **1984**, *98* (4), 1163–9.
- (13) Singer, K. L.; Mostov, K. E. Dimerization of the polymeric immunoglobulin receptor controls its transcytotic trafficking. *Mol. Biol. Cell* **1998**, *9* (4), 901–5.
- (14) Muro, S.; Wiewrodt, R.; Thomas, A.; Koniaris, L.; Albelda, S. M.; Muzykantov, V. R.; Koval, M. A novel endocytic pathway induced by clustering endothelial ICAM-1 or PECAM-1. *J. Cell Sci.* **2003**, *116* (Pt 8), 1599–609.
- (15) Muro, S.; Gajewski, C.; Koval, M.; Muzykantov, V. R. ICAM-1 recycling in endothelial cells: a novel pathway for sustained intracellular delivery and prolonged effects of drugs. *Blood* **2005**, *105* (2), 650–8.
- (16) Serrano, D.; Bhowmick, T.; Chadha, R.; Garnacho, C.; Muro, S. Intercellular adhesion molecule 1 engagement modulates sphingomyelinase and ceramide, supporting uptake of drug carriers by the vascular endothelium. *Arterioscler. Thromb. Vasc. Biol.* **2012**, *32* (5), 1178–85.
- (17) Bhowmick, T.; Berk, E.; Cui, X.; Muzykantov, V. R.; Muro, S. Effect of flow on endothelial endocytosis of nanocarriers targeted to ICAM-1. *J. Controlled Release* **2012**, *157* (3), 485–92.
- (18) Calderon, A. J.; Muzykantov, V.; Muro, S.; Eckmann, D. M. Flow dynamics, binding and detachment of spherical carriers targeted to ICAM-1 on endothelial cells. *Biorheology* **2009**, *46* (4), 323–41.
- (19) Muro, S. Intercellular Adhesion Molecule-1 and Vascular Cell Adhesion Molecule-1. In *Endothelial Biomedicine*, 1st ed.; Aird, W. C., Ed.; Cambridge University Press: New York, 2007; pp 1058–1070.
- (20) Murciano, J.-C.; Muro, S.; Koniaris, L.; Christofidou-Solomidou, M.; Harshaw, D. W.; Albelda, S. M.; Granger, D. N.; Cines, D. B.; Muzykantov, V. R. ICAM-directed vascular immunotargeting of antithrombotic agents to the endothelial luminal surface. *Blood* **2003**, *101* (10), 3977–84.
- (21) Hsu, J.; Serrano, D.; Bhowmick, T.; Kumar, K.; Shen, Y.; Kuo, Y. C.; Garnacho, C.; Muro, S. Enhanced endothelial delivery and biochemical effects of alpha-galactosidase by ICAM-1-targeted nanocarriers for Fabry disease. *J. Controlled Release* **2011**, *149* (3), 323–31.
- (22) Garnacho, C.; Dhami, R.; Simone, E.; Dziubla, T.; Leferovich, J.; Schuchman, E. H.; Muzykantov, V.; Muro, S. Delivery of acid sphingomyelinase in normal and Niemann-Pick disease mice using intercellular adhesion molecule-1-targeted polymer nanocarriers. *J. Pharmacol. Exp. Ther.* **2008**, *325* (2), 400–8.
- (23) Muro, S. Strategies for delivery of therapeutics into the central nervous system for treatment of lysosomal storage disorders. *Drug Delivery Transl. Res.* **2012**, *2* (3), 169–86.
- (24) Hamilton, A. J.; Huang, S. L.; Warnick, D.; Rabbat, M.; Kane, B.; Nagaraj, A.; Klegerman, M.; McPherson, D. D. Intravascular

- ultrasound molecular imaging of atheroma components in vivo. *J. Am. Coll. Cardiol.* **2004**, *43* (3), 453–60.
- (25) Weller, G. E.; Villanueva, F. S.; Tom, E. M.; Wagner, W. R. Targeted ultrasound contrast agents: in vitro assessment of endothelial dysfunction and multi-targeting to ICAM-1 and sialyl Lewis x. *Biotechnol. Bioeng.* **2005**, *92* (6), 780–8.
- (26) Choi, K. S.; Kim, S. H.; Cai, Q. Y.; Kim, S. Y.; Kim, H. O.; Lee, H. J.; Kim, E. A.; Yoon, S. E.; Yun, K. J.; Yoon, K. H. Inflammation-specific T1 imaging using anti-intercellular adhesion molecule 1 antibody-conjugated gadolinium diethylenetriaminepentaacetic acid. *Mol. Imaging* **2007**, *6* (2), 75–84.
- (27) Zhang, N.; Chittasupho, C.; Duangrat, C.; Siahaan, T. J.; Berkland, C. PLGA nanoparticle-peptide conjugate effectively targets intercellular cell-adhesion molecule-1. *Bioconjugate Chem.* **2008**, *19* (1), 145–52.
- (28) Gunawan, R. C.; Auguste, D. T. Immunoliposomes that target endothelium in vitro are dependent on lipid raft formation. *Mol. Pharmaceutics* **2010**, *7* (5), 1569–75.
- (29) Park, S.; Kang, S.; Veach, A. J.; Vedvyas, Y.; Zarnegar, R.; Kim, J. Y.; Jin, M. M. Self-assembled nanoplatform for targeted delivery of chemotherapy agents via affinity-regulated molecular interactions. *Biomaterials* **2010**, *31* (30), 7766–75.
- (30) Barreiro, O.; Yanez-Mo, M.; Serrador, J. M.; Montoya, M. C.; Vicente-Manzanares, M.; Tejedor, R.; Furthmayr, H.; Sanchez-Madrid, F. Dynamic interaction of VCAM-1 and ICAM-1 with moesin and ezrin in a novel endothelial docking structure for adherent leukocytes. *J. Cell Biol.* **2002**, *157* (7), 1233–45.
- (31) Carman, C. V.; Jun, C.-D.; Salas, A.; Springer, T. A. Endothelial cells proactively form microvilli-like membrane projections upon intercellular adhesion molecule 1 engagement of leukocyte LFA-1. *J. Immunol.* **2003**, *171* (11), 6135–44.
- (32) Hopkins, A. M.; Baird, A. W.; Nusrat, A. ICAM-1: targeted docking for exogenous as well as endogenous ligands. *Adv. Drug Delivery Rev.* **2004**, *56* (6), 763–78.
- (33) Greve, J. M.; Davis, G.; Meyer, A. M.; Forte, C. P.; Yost, S. C.; Marlor, C. W.; Kamarck, M. E.; McClelland, A. The major human rhinovirus receptor is ICAM-1. *Cell* **1989**, *56* (5), 839–47.
- (34) Rieder, E.; Gorbalenya, A. E.; Xiao, C.; He, Y.; Baker, T. S.; Kuhn, R. J.; Rossmann, M. G.; Wimmer, E. Will the polio niche remain vacant? *Dev Biol.* **2001**, *105*, 111–22 discussion 149–50.
- (35) Stein, B. S.; Sussman, H. H. Demonstration of two distinct transferrin receptor recycling pathways and transferrin-independent receptor internalization in K562 cells. *J. Biol. Chem.* **1986**, *261* (22), 10319–31.
- (36) Anderson, R. G.; Brown, M. S.; Beisiegel, U.; Goldstein, J. L. Surface distribution and recycling of the low density lipoprotein receptor as visualized with antireceptor antibodies. *J. Cell Biol.* **1982**, *93* (3), 523–31.
- (37) Jo, J. H.; Kwon, M. S.; Choi, H. O.; Oh, H. M.; Kim, H. J.; Jun, C. D. Recycling and LFA-1-dependent trafficking of ICAM-1 to the immunological synapse. *J. Cell. Biochem.* **2010**, *111* (5), 1125–37.
- (38) Muro, S.; Dziubla, T.; Qiu, W.; Leferovich, J.; Cui, X.; Berk, E.; Muzykantov, V. R. Endothelial targeting of high-affinity multivalent polymer nanocarriers directed to intercellular adhesion molecule 1. *J. Pharmacol. Exp. Ther.* **2006**, *317* (3), 1161–9.
- (39) Hsu, J.; Northrup, L.; Bhowmick, T.; Muro, S. Enhanced delivery of alpha-glucosidase for Pompe disease by ICAM-1-targeted nanocarriers: comparative performance of a strategy for three distinct lysosomal storage disorders. *Nanomedicine* **2012**, *8* (5), 731–9.
- (40) Muro, S.; Schuchman, E. H.; Muzykantov, V. R. Lysosomal enzyme delivery by ICAM-1-targeted nanocarriers bypassing glycosylation- and clathrin-dependent endocytosis. *Mol. Ther.* **2006**, *13* (1), 135–41.
- (41) Muro, S.; Muzykantov, V. R.; Murciano, J. Characterization of endothelial internalization and targeting of antibody-enzyme conjugates in cell cultures and in laboratory animals. In *Methods in Molecular Biology. Bioconjugation Protocols*; Niemeyer, C. M., Ed.; Humana Press: Totowa, NJ, 2004; Vol. 283, pp 21–36.
- (42) Muro, S.; Cui, X.; Gajewski, C.; Murciano, J.-C.; Muzykantov, V. R.; Koval, M. Slow intracellular trafficking of catalase nanoparticles targeted to ICAM-1 protects endothelial cells from oxidative stress. *Am. J. Physiol. Cell Physiol.* **2003**, *285* (5), C1339–47.
- (43) Diamond, M. S.; Staunton, D. E.; Marlin, S. D.; Springer, T. A. Binding of the integrin Mac-1 (CD11b/CD18) to the third immunoglobulin-like domain of ICAM-1 (CD54) and its regulation by glycosylation. *Cell* **1991**, *65* (6), 961–71.
- (44) Norris, S. H.; Johnstone, J. N.; DeLeon, R.; Rothlein, R. A competitive ELISA for the anti-intercellular adhesion molecule-1 (anti-ICAM-1) binding activity of monoclonal antibody R6.5 in serum. *J. Pharm. Biomed. Anal.* **1991**, *9* (3), 211–7.
- (45) Garnacho, C.; Shuvaev, V.; Thomas, A.; McKenna, L.; Sun, J.; Koval, M.; Albelda, S.; Muzykantov, V.; Muro, S. RhoA activation and actin reorganization involved in endothelial CAM-mediated endocytosis of anti-PECAM carriers: critical role for tyrosine 686 in the cytoplasmic tail of PECAM-1. *Blood* **2008**, *111* (6), 3024–33.
- (46) van IJzendoorn, S. C. Recycling endosomes. *J. Cell Sci.* **2006**, *119* (Pt 9), 1679–81.
- (47) Zeigerer, A.; Lampson, M. A.; Karylowski, O.; Sabatini, D. D.; Adesnik, M.; Ren, M.; McGraw, T. E. GLUT4 retention in adipocytes requires two intracellular insulin-regulated transport steps. *Mol. Biol. Cell* **2002**, *13* (7), 2421–35.
- (48) Lock, J. G.; Stow, J. L. Rab11 in recycling endosomes regulates the sorting and basolateral transport of E-cadherin. *Mol. Biol. Cell* **2005**, *16* (4), 1744–55.
- (49) Fabbri, M.; Di Meglio, S.; Gagliani, M. C.; Consonni, E.; Molteni, R.; Bender, J. R.; Tacchetti, C.; Pardi, R. Dynamic partitioning into lipid rafts controls the endo-exocytic cycle of the alphaL/beta2 integrin, LFA-1, during leukocyte chemotaxis. *Mol. Biol. Cell* **2005**, *16* (12), 5793–803.
- (50) Ullrich, O.; Reinsch, S.; Urbe, S.; Zerial, M.; Parton, R. G. Rab11 regulates recycling through the pericentriolar recycling endosome. *J. Cell Biol.* **1996**, *135* (4), 913–24.
- (51) Muro, S. A DNA-device that mediates selective endosomal escape and intracellular delivery of drugs and biologicals. *Adv. Funct. Mater.* **2014**, *24* (19), 2899–2906.
- (52) Mastrobattista, E.; Storm, G.; van Bloois, L.; Reszka, R.; Bloemen, P. G.; Crommelin, D. J.; Henricks, P. A. Cellular uptake of liposomes targeted to intercellular adhesion molecule-1 (ICAM-1) on bronchial epithelial cells. *Biochim. Biophys. Acta* **1999**, *1419* (2), 353–63.
- (53) Powelka, A. M.; Sun, J.; Li, J.; Gao, M.; Shaw, L. M.; Sonnenberg, A.; Hsu, V. W. Stimulation-dependent recycling of integrin beta1 regulated by ARF6 and Rab11. *Traffic* **2004**, *5* (1), 20–36.
- (54) Mamdouh, Z.; Chen, X.; Pierini, L. M.; Maxfield, F. R.; Muller, W. A. Targeted recycling of PECAM from endothelial surface-connected compartments during diapedesis. *Nature* **2003**, *421* (6924), 748–53.
- (55) Millán, J.; Hewlett, L.; Glyn, M.; Toomre, D.; Clark, P.; Ridley, A. J. Lymphocyte transcellular migration occurs through recruitment of endothelial ICAM-1 to caveola- and F-actin-rich domains. *Nat. Cell Biol.* **2006**, *8* (2), 113–23.
- (56) Weller, G. E.; Wong, M. K.; Modzelewski, R. A.; Lu, E.; Klibanov, A. L.; Wagner, W. R.; Villanueva, F. S. Ultrasonic imaging of tumor angiogenesis using contrast microbubbles targeted via the tumor-binding peptide arginine-arginine-leucine. *Cancer Res.* **2005**, *65* (2), 533–9.
- (57) Garnacho, C.; Serrano, D.; Muro, S. A fibrinogen-derived peptide provides intercellular adhesion molecule-1-specific targeting and intraendothelial transport of polymer nanocarriers in human cell cultures and mice. *J. Pharmacol. Exp. Ther.* **2012**, *340* (3), 638–47.
- (58) Calderon, A. J.; Bhowmick, T.; Leferovich, J.; Burman, B.; Pichette, B.; Muzykantov, V.; Eckmann, D. M.; Muro, S. Optimizing endothelial targeting by modulating the antibody density and particle concentration of anti-ICAM coated carriers. *J. Controlled Release* **2011**, *150* (1), 37–44.

- (59) Muro, S. New biotechnological and nanomedicine strategies for treatment of lysosomal storage disorders. *Wiley Interdiscip. Rev. Nanomed. Nanobiotechnol.* **2010**, *2* (2), 189–204.
- (60) Muro, S.; Garnacho, C.; Champion, J. A.; Leferovich, J.; Gajewski, C.; Schuchman, E. H.; Mitragotri, S.; Muzykantov, V. R. Control of endothelial targeting and intracellular delivery of therapeutic enzymes by modulating the size and shape of ICAM-1-targeted carriers. *Mol. Ther.* **2008**, *16* (8), 1450–8.
- (61) Villanueva, F. S.; Jankowski, R. J.; Klibanov, S.; Pina, M. L.; Alber, S. M.; Watkins, S. C.; Brandenburger, G. H.; Wagner, W. R. Microbubbles targeted to intercellular adhesion molecule-1 bind to activated coronary artery endothelial cells. *Circulation* **1998**, *98* (1), 1–5.
- (62) Haug, C. E.; Colvin, R. B.; Delmonico, F. L.; Auchincloss, H., Jr.; Tolkoff-Rubin, N.; Preffer, F. I.; Rothlein, R.; Norris, S.; Scharschmidt, L.; Cosimi, A. B. A phase I trial of immunosuppression with anti-ICAM-1 (CD54) mAb in renal allograft recipients. *Transplantation* **1993**, *55* (4), 766–72 discussion 772–3..
- (63) Stefanelli, T.; Malesci, A.; De La Rue, S. A.; Danese, S. Anti-adhesion molecule therapies in inflammatory bowel disease: touch and go. *Autoimmun. Rev.* **2008**, *7* (5), 364–9.